Crystal phase engineered quantum wells in ZnO nanowires

Volodymyr Khranovskyy, Alexey M. Glushenkov, Y Chen, A Khalid, H Zhang, Lars Hultman, Bo Monemar and Rositsa Yakimova

Original Publication:

Volodymyr Khranovskyy, Alexey M. Glushenkov, Y Chen, A Khalid, H Zhang, Lars Hultman, Bo Monemar and Rositsa Yakimova, Crystal phase engineered quantum wells in ZnO nanowires, 2013, Nanotechnology, (24), 21.
http://dx.doi.org/10.1088/0957-4484/24/21/215202

Crystal Phase Engineered Quantum Wells in ZnO Nanowires

V. Khranovskyy[1,a], A. M. Glushenkov[2], Y. Chen[2], A. Khalid[3], H.Zhang[3], L. Hultman[1], B. Monemar[1] and R. Yakimova[1]

[1]Linköping University, Department of Physics, Chemistry, and Biology (IFM), 583 81 Linköping, Sweden

[2]Institute for Frontier Materials (IFM), Deakin University, Waurn Ponds, 3216 Victoria, Australia

[3]School of Physics and Centre for Research on Adaptive Nanostructures and Nanodevices (CRANN), Trinity College Dublin, Dublin 2, Ireland

Corresponding author: Dr. Volodymyr Khranovskyy, volkh@ifm.liu.se,

Abstract

We report the fabrication of quantum wells in ZnO nanowires (NWs) by crystal phase engineering approach. Basal plane stacking faults (BSF) in wurtzite structure can be considered as a minimal segment of zinc blende. Due to the existing band offsets at wurtzite (WZ) / zinc blende (ZB) materials interface incorporation of BSF of high density into ZnO NWs results in type II band alignment. Thus, the BSF structure acts as a quantum well for electrons and a potential barrier for holes in the valence band. We have studied the photoluminescence (PL) properties of ZnO NWs containing high concentration of BSF in comparison to high quality ZnO NWs of pure wurtzite structure. It is revealed that BSF form quantum wells in WZ ZnO nanowires, providing an additional luminescence peak at 3.329 eV at 4 K. The luminescence mechanism is explained as indirect exciton transition due to the recombination of electrons in the QW conduction band to holes localized near the BSF. The binding energy of electrons is found to be around 100 meV, while the excitons are localised with binding energy of holes ~ 5 meV, which is due to the coupling of BSF, which form QW-like structures.

1. Introduction

Semiconductor nanowires (NWs) are considered as an important technology for future advanced devices [1]. Carrier confinement in semiconductor nanostructures, namely, quantum wells (QWs) or quantum dots (QDs) has the well-known advantage of increasing radiative recombination efficiency, making them of particular interest for optoelectronic applications. Many of recent reports demonstrate significant progress toward engineering of the properties of semiconductor NWs via respective doping creating QD or QW [2]. Crystal phase engineering is an alternative approach, which practically enables engineering of the electronic structure of a single material [3,4]. Due to the existing band offsets at wurtzite (WZ) / zinc blende (ZB) materials interface, the hetero-interface WZ/ZB/WZ can define a QW in a single material. While growing of such a structure in a NW allows confinement of charges in two other dimensions, forming a crystal phase QD [3]. Crystal phase engineering has several advantages over traditional approach, e. g. an atomically sharp interface is provided and no alloying or strain is induced [4]. Earlier, Pemasiri et al [5] demonstrated that ZB/WZ stacking provides type-II band alignment for InP NWs, using time-resolved μPL. Spirkoska et al [6] demonstrated in Ga-nucleated GaAs NWs that WZ/ZB polytypism can lead to type-II ZB QD formation, using μPL and cathodoluminescence. Finally, Akopian et al. demonstrated unambiguously the possibility for single-photon emission from a crystal phase QD [7].

ZnO is a wide direct band gap semiconductor (E_g = 3.36 eV), with large exciton binding energy (~ 60 meV), which makes it a potential material for design of high-efficiency optoelectronic and photonic devices [7]. Both, bulk material and NWs of ZnO exhibit single phase WZ crystal structure at normal conditions. However, at certain conditions stacking faults (SF) are observed in ZnO [8] similarly to other wurtzite-type semiconductors, like GaN [9] etc. SF may be of different types: basal plane SF, prismatic SF, partial dislocations-terminating basal-plane SF etc. Among them, basal plane stacking faults (BSF) are the most common type (~90%)[9]. BSFs in wurtzite-structure ZnO, can be considered as a sheet of zinc blende structure (ZB) embedded in the parent

crystal [10]. Due to the smaller bandgap of the ZB modification, these BSFs form *perfect* ZB-like quantum wells in a WZ matrix [11]. Thus, once the formation of SF can be "engineered", it could transform a challenging defect-related problem into a groundbreaking advantage for crystal phase band gap engineering [4]. This approach was recently described for the design of "perfectly imperfect" nanowires [12].

As a structural defect type I, stacking faults in a wurtzite crystal can be thought as a thin layer of zinc blende structure with a thickness of a few nanometres. Figure 1 represents a schematic of the minimal ZB segment inserted into WZ phase. The term stacking faults means that there is a local interruption in the regular sequence and that the latter continues at the same manner after the SF. The respective stacking sequence in WZ is described as ABAB… and in ZB as ABCABC…. Due to the smaller band gap of ZB ZnO, such insertion into WZ matrix creates the quantum well. According to *ab initio* calculations [13], the BSF forms a quantum well/like region with negative band offsets in the conduction band minimum (CBM) and the valence band maximum with respect to those of the wurtzite barriers. Thus, the BSF structure would act as a quantum well for electrons and a potential barrier for holes in the valence band. The valence band offset for WZ and ZB ZnO has been calculated by Yan et al [13]: $\Delta E = 0.037$ eV. The band gap calculated for WZ ZnO is 0.11 eV larger than that for ZB ZnO and the conduction band offset for WZ and ZB was predicted to be 0.147 eV. Thus the band alignment is type II: the electronic states at the conduction band minima are localized mainly in the ZB region, while those at the valence band minima are preferentially localized in the WZ region. This band alignment indicates that the mixed WZ/ZB/WZ regions exhibit quantum-well-like features. Thus, carrier localization in the quantum-well-like regions is expected to impact the electronic and transport properties of the material.

We have studied the photoluminescence (PL) properties of ZnO NWs containing high concentration of BSF in comparison to high quality ZnO NWs of pure wurtzite structure. It is revealed that BSF form quantum wells in WZ ZnO nanowires, providing an additional luminescence peak at 3.329 eV at 4 K. The observed peak is explained as indirect exciton transition due to the recombination of electrons in the QW conduction band to holes localized near BSF. The binding energy of electrons is estimated to be

around 100 meV, while the excitons are found to be localised with binding energy of holes ~ 5 meV, which is due to the coupling of BSF, which form QW-like structures.

2. Experimental details

The NWs containing high concentration of BSF were prepared by thermal evaporation of a ball milled ZnO powder at ~ 1300 °C inside of a conventional tube furnace [14]. Ar gas with a flow of 0.4 l min^{-1} was used as a carrier gas to transfer ZnO vapor from the central hot zone of the furnace to a cooler zone, where a Si substrate was placed. A layer of nanowires was formed on the Si substrate located at 17 –20 cm from the vapor source (the temperature was estimated to be ~250–400 °C) after 1 h. High quality ZnO nanowires (further mentioned as WZ NWs), grown on Si substrate by APMOCVD [15] at 700 °C were used as a reference.

The structure of the obtained nanowires was studied by using a Carl Zeiss Orion Plus helium-ion microscope. The crystal features of ZnO nanowires were evaluated by high resolution transmission electron microscopy (HR TEM) using an FEI Titan microscope operating at 300 kV. The light emission features of the samples were studied by a micro-photoluminescence setup. Excitation was performed by a frequency doubled Nd:YVO laser as a continuous wave excitation source, giving a wavelength λ = 266 nm. The laser beam was focused by a UV lens, providing an excited area around 1.5 μm in diameter. The emitted luminescence was collected and mirrored into a single grating 0.45 m monochromator equipped with a liquid nitrogen cooled Si-CCD camera with a spectral resolution of ~ 0.1 meV. Via control of the laser transmittance the power excitation density was kept ~10 W/cm^2. The low temperature PL study was performed at 4 K by helium cooling of the cold-finger where the samples were placed. Via decreasing the liquid He flow and local heating of the sample holder a temperature dependent PL study was performed in the range from 4 to 300 K.

3. Results and discussion

Recently, Glushenkov *et al* [14] reported the fabrication the ZnO NWs with corrugated side facets, which was explained as due to high concentration of the stacking faults in the NWs. We have studied these NWs by helium ion microscopy and TEM in

order to reveal the density of the BSF (Figure 2). The low magnification helium-ion microscopy image (Figure 2(a)) reveals a spool of NWs covering the Si substrate, whereas an individual NW is shown in Figure 2(b). In order to observe BSF by TEM, the NWs were tilted to align the electron beam with their [2 $\bar{1}$ $\bar{1}$ 0] crystallographic direction. Figure 2(c) shows a TEM image of an individual ZnO NW, and the contrast of basal stacking faults perpendicular to the general [0001] growth direction of the NW is apparent. It is observed, that the BSF are quasiperiodically inserted into WZ ZnO and their density varies along the length of the nanowire. We have studied detail structure of the NWs on the area, marked by square on Figure 2(c) by HR TEM. It shows that the NWs have single crystalline wurtzite structure, where the BSF are inserted inhomogeneously – marked by arrows in Figure 2(d). It should be noticed that different NWs possess different density of BSF. Some of them were found to comprise extremely high density of BSF, penetrating them every 3 -5 nm, while others (like that one depicted on Figure 2(c,d)) have rather large BSF free areas - up to 20 – 30 nm. In parallel we have studied the reference sample of high quality ZnO NWs for comparison. HR TEM study (not shown here) confirmed that the references NWs are a single crystalline wurtzite ZnO material without any SFs or other defects.

Optical studies of the NWs have been performed earlier by cathodoluminescence [16], but only at room temperature. The room temperature CL spectrum of nanowires is dominated by a wide visible emission, centred at 510 nm (2.43 eV), while the NBE emission is hardly observable. Therefore, we investigate the LT PL spectrum of the NWs with BSF in comparison to reference sample of pure wurtzite ZnO NWs.

The wide range LT PL spectra of the samples are different in terms of available peaks and their spectral position respectively. The LT PL spectrum (4 K) of ZnO NWs with BSF (marked as 1 on Figure 3) consists of two main regions. On the low-energy side the wide and intense deep level emission DLE is present. This emission has been observed from the lowest measured temperatures up to room temperature. This emission may be due to the point defects (oxygen vacancies, zinc interstitials and their complexes [17], which could be introduced during growth at high supersaturation. However, we will not focus on it in this article. The high energy side of the spectrum displays the near band edge NBE emission, which comprises a number of peaks (Figure 3(b) marked as 1).

Analysis of the NBE peaks suggests that there is a neutral donor bound exciton peak (D^0X) at 3.366 eV, and an independent peak at 3.329 eV, which we attribute to the emission due to stacking faults. This is a luminescence feature, independent of the free or neutral donor bound excitonic recombination. Additionally, the spectrum is complicated by multiple longitudinal replicas of the present peaks (1^{st}, 2^{nd}, and up to 3^{rd} LO) separated between each other by ~72 meV. The coupling mechanism of LO phonons to the BSF recombination is apparently similar to the coupling of LO phonons to free excitons [18]. However, the rather unusual symmetry and width of the peaks can be explained by possible overlapping with other existing peaks. The BSF peak may thus be enhanced by two electron satellites (TES) of the D^0X emission, while its peak asymmetry may be caused by the 1^{st} LO of D^0X, and the 2^{nd} LO replica of BSF is unusually strong due to possible overlap with a separate DAP transition.

The LT PL spectrum of reference wurtzite ZnO NWs (marked as 2 on Figure 3(a, b)) is solely dominated by the NBE emission, which consists of several closely located peaks at 3.3737 eV, 3.3693 eV and 3.3645 eV, attributed to the donors bound exciton emission (D^0X) [19, 20]. No other peaks were observed, unambiguously suggesting that the peak at 3.329 eV, observed for BSFs reach sample, is related to the BSF emission.

While it is common knowledge that the D^0X emission is of excitonic type, the nature of BSF emission has to be clarified. We have measured the temperature-dependent μ-PL. Figure 4(a) displays the NBE part of PL spectra for the ZnO nanostructures taken at temperatures between 10 and 290 K. Note that the spectra presented in Figure 4 were taken with as low excitation power as 10 mW/cm^2 in order to minimize laser heating. With temperature increase both the spectral location and the intensities of the peaks are changing. At low cryogenic temperatures the bound exciton emission is the dominant radiative channel, whereas at the higher temperatures the free exciton emission usually takes over. Thus, the D^0X, being dominant at 4 K is rapidly decreased with T increase. While FX emission takes over after ~40 K, becoming dominant with further T increase. This is a typical D^0X to FX interplay behavior [20]. The BSF emission peak exists up to 180 K, and becomes further shadowed by the growing FX emission. Interestingly, the LO phonon replica intensities in the low-temperature region are not well ordered, confirming the fact that these peaks are additionally complicated by overlap with TES or DAP.

However, in the higher-temperature region, the LO replicas of the main peaks (BSF and FX) behaves trivially, being widened, merged together and therefore not resolvable above 180 K. In order to clarify the mutual relation of the emissions, we have plotted the relative intensity of the main peak's D^0X-FX, BSF, and the DLE bands (Figure 4(b)). At low temperatures the observed emissions represent mutually competing carrier recombination processes. Analysing the intensity of the specific peak with the temperature, it is evident, that in the temperature range 50 – 150 K both D^0X emission and FX emissions are quenched in favour of the enhanced DLE emission.

In order to clarify unambiguously the peaks assignment, we have additionally performed a power dependent PL study. The PL spectra were acquired at different excitation energies (P_{exc}) ranging from 2 to 400 mW/cm^2 at 4 K. The FX and BSFs peaks were fitted by Gaussian and their spectral integral intensities as functions of excitation power were determined. Both FX and BSF emissions follow a power low $I = P^n$, with the n values 1.19 and 1.39, respectively. For a bound or free exciton emission, the value of the exponent n should be in range 1 – 2 [21]. Therefore, both observed emission peaks are due to excitonic transitions.

A small red shift with excitation power increase has been observed for the energy position of both peaks. However, a careful analysis of the dependencies reveals that both FX and BSF peaks shift simultaneously, which implies that the observed feature is due to the local laser heating of the irradiated nanostructures. This explanation is reasonable, taking into account the small size of the nanowires and a negligible heat exchange with the substrate.

Temperature increase resulted in energy shifts of D^0X (at low temperature region) and FX (that became dominant at higher temperatures) as well as of the BSF emission. Peak energies of NBE, including D^0X, FX and BSF, are plotted as a function of temperature in Figure 4(c). It is clear that the peaks develop in different ways: the D^0X peak red shifts constantly from its initial position at 4 K, being then taken over by FX. Then FX peak energy monotonically decreases with T.

By fitting the experimental data of the FX peak energy position within the observable temperature limits by the Varshni expression (red and blue lines on Fig. 4c) we have obtained the value of free exciton energy $E_{FX}(0)$ = 3.3742 eV at T=0 K [22]:

$E(T) = E(0) - (\alpha T^2/(T+\beta))$, where α and β are the fitting parameters. The value of β is Debye temperature [23, 24] and was found to be 790 K. The value of α, was calculated to be 8.5×10^{-4} eV/K, which agrees well with the one reported for free excitons (see, e. g., Ref. 25). The same fitting procedure has been applied to the BSF experimental data, giving the estimated energy of BSF at 0 K $E_{BSF}(0) = 3.3339$ eV. Having $E_{FX}(0) = 3.3742$ eV and assuming the exciton binding energy 60 meV, we obtain the ZnO band gap energy $E_g = 3.4342$ eV. Then the QW electron binding energy can be estimated as $E_{QW} = E_g - 3.3339 = 0.1003$ eV, or ~ 0.10 eV.

The energy of the BSF emission shifts differently from the FX emission as a function of temperature: first it undergoes a blue shift from 3.329 eV to 3.332 eV as the temperature increases from 4 to 40 K and then it redshifts with further temperature increase (Figure 4(c)). Fitting the peak energy of the BSF emission above 40 K by the Varshni formula yields E(0) = 3.3339 eV, which gives a blue shift ~ 5 meV with respect to the measured 3.329 eV at 4 K.

We suggest the following recombination mechanism: the observed high energy PL peak at 3.366 eV corresponds to donor bound exciton transition of WZ ZnO (Figure 5), while the peak at 3.329 is due to the recombination of the confined indirect excitons in the BSF. This transition is due to the recombination of the electrons captured in the quantum wells of the BSF and the holes confined at the interface of BSF and wurtzite structure via attractive Coulomb interaction [26]. The periodical multiple BSF could be considered as a coupled quantum well structure in which the coupling effect of the electron wave function may be responsible for the broadening of the PL peak. Similar phenomena of exciton localization have earlier been reported for the case of BSF in GaN [4], InGaN [27], AlGaN [28] as well as single and multiple quantum wells structures [29]. The hole localization energy (~5 meV) is related to the present BSF density and could be explained due to a weak coupling between them (as in comparison to 19 meV in Ref. 10), thus forming the multiple QW. However, in the studied nanowires, the BSF are distributed along the growth direction (c-axis) with rather large separation (Figure 2(c,d)). Therefore, it is rather questionable that the holes wave functions are overlapped. Taking into account as small localization energy as 5 meV, it is more probable that the hole localization is due to band bending as a result of a strong polarization field, that exist

in polar wurtzite semiconductors, like GaN and ZnO. However, this question requires more investigations.

4. Conclusion

We demonstrated the design of quantum wells in ZnO NWs by crystal phase engineering. Via incorporation of the BSF into wurtzite ZnO a clear heterostructure with sharp WZ/ZB/WZ interface is obtained. Due to smaller band gap of ZB in comparison to WZ, the type II band alignment is provided: every BSF act as a quantum well for electrons and a potential barrier for holes in the valence band. The fabricated samples demonstrate the specific PL peak at 3.329 eV at 4 K, which is a result of an indirect exciton transition from electrons of the QW in the conduction band recombining with holes, localized at BSF. The binding energy of QW electrons is estimated to be ~100 meV. It is also found that excitons are localized with the binding energy of holes of ~t 5 meV. This is explained as a consequence of the coupling of BSF, which form quantum well-like structures.

Acknowledgements

We acknowledge the Linköping Linnaeus Initiative for Novel Functional Materials (LiLi-NFM) for the support of this work.

References

[1] Yang P, Yan R, Fardy T, 2010 *Nano Lett.* **10** 1529.
[2] Reitzenstein S and Forchel A, 2010 *J. Phys. D: Appl. Phys.* **43** 033001-1; Michler P 2000 *Science* **290** 2282
[3] Akopian N, Patriarche G, Liu L, Harmand J-C and Zwiller V 2010 *Nano Lett.* **10** 1198
[4] Caroff P, Bolinsson J and Johansson J 2010 *IEEE Journal of Selected Topics in Quantum Electronics* **17** 829
[5] Pemasiri K, Montazeri M, Gass R, Smith L M, Jackson H E, Yarrison-Rice J, Paiman S, Gao Q, Tan H H, Jagadish C, Zhang X and Zou J 2009 *Nano Lett.* **9** 648
[6] Spirkoska D, Arbiol J, Gustafsson A, Conesa-Boj S, Glas F, Zardo I, Heigoldt M, Gass M H, Bleloch A L, Estrade S, Kaniber M, Rossler J, Peiro F, Morante J R, Abstreiter G, Samuelson L, Fontcuberta i Morral1 A 2009 *Phys. Rev. B* **80** 245325
[7] Djurisic A, Ng M C, Chen X. Y 2010 *Progr. Quant. Electr.* **34** 191–259

[8] Thonke K, Schirra M, Schneider R, Reiser A, Prinz G M, Feneberg M, Biskupek J, Kaiser U, Sauer R 2009 *Microelectronics J* **40** 210-214
[9] Paskov P P, Schifano R, Monemar B, Paskova T, Figge S and Hommel D 2005 *J. Appl. Phys.* **98** 093519
[10] Yang S, Kuo C, Liu W-R, Lin B H, Hsu H-C and Hsieh W F 2012 *Appl. Phys. Lett.* **100** 101907
[11] Lähnemann J, Brandt O, Jahn U, Pfuller C, Roder C, Dogan P, Grosse F, Belabbes A, Bechstedt F, Trampert A, and Geelhaar L2012 *Phys. Rev. B* **86** 081302(R)
[12] Perfectly imperfect, 2010 *Nature Nanotechnology* **5** 311
[13] Yan Y, Dalpian G M, Al-Jassim M M, and Wei S-H 2004 *Phys. Rev. B* **70** 193206
[14] Glushenkov A, Zhang H, Zou J, Lu G Q, Chen Y 2008 *J. Cryst. Growth* **310** 3139 - 3143
[15] Khranovskyy V, Yakimova R 2012 *Phys. B: Cond. Matter* **407** 1533
[16] Glushenkov A, Zhang H Z, Zou J, Lu G Q, Chen Y 2007 *Nanotechnology* **18** 175604
[17] Khranovskyy V, Lazorenko V, Lashkarev G, Yakimova R 2012 *J. Lumin.* **132** 2643
[18] Segall B, Mahan G F 1968 *Phys. Rev.* **171** 935
[19] Djurisic A, Ng A M C, Chen X Y 2010 *Progr. Quant. Electr.* **34** 191–259
[20] Meyer B K 2003 *Physica B* **201** 340–342; Khranovskyy V, Tsiaoussis I, Hultman L and Yakimova R 2011 *Nanotechnology* **22** 185603
[21] Schmidt T, Lischka K, Zulehner W, 1992 *Phys. Rev. B.* **45** 8989
[22] Varshni Y P 1967 *Physica* **34** 149
[23] Hur T-B, Jeen G S, Hwang Y-H and Kim H-K 2003 *J. Appl. Phys.* **94** 5787
[24] Wang L and Giles N C 2003 *J. Appl. Phys.* **94** 973
[25] Shimomura T, Kim D and Nakayama M 2005 *J. Lumin.* **112** 191
[26] Rebane Y T, Shreter Y G and Albrecht M 1997 *Phys. Status Solidi A* **164** 141
[27] Li Q, Xu S J, Cheng W C, Xie M H, Tong S. Y, Chen C M and Yang H 2001 *Appl. Phys. Lett.* **79** 1810
[28] Chung S J, Senthil Kumar M, Lee H J, and Suh E-K 2004 *J. Appl. Phys.* **95** 3565
[29] Ramaiah K S,Su Y K, Chang S J, Kerr B, Liu H P and Chen I G 2004 *Appl. Phys. Lett.* **84** 3307

List of figures

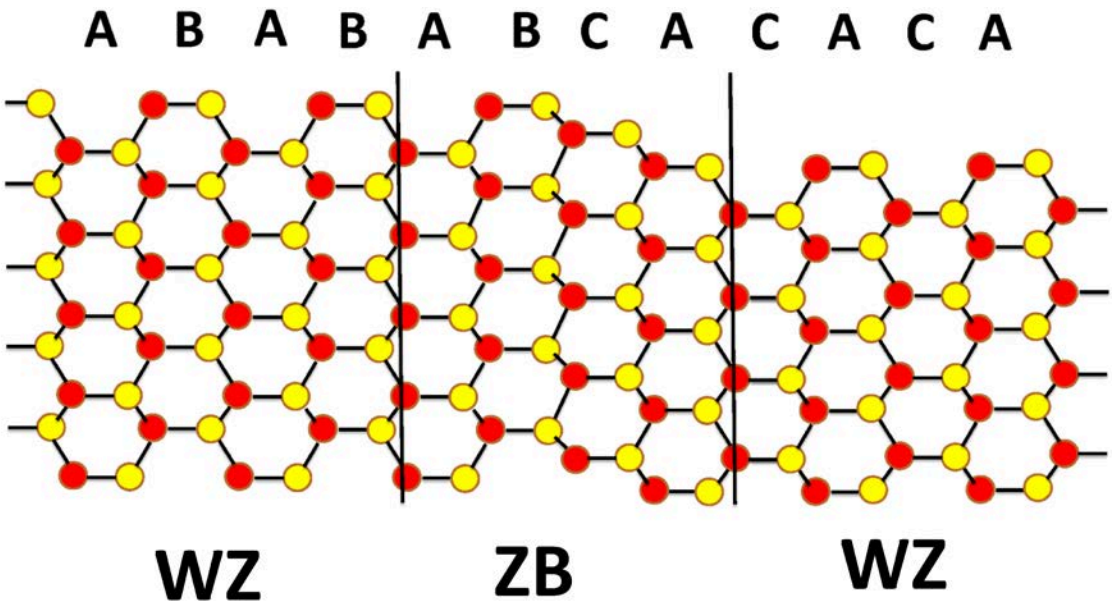

Fig. 1

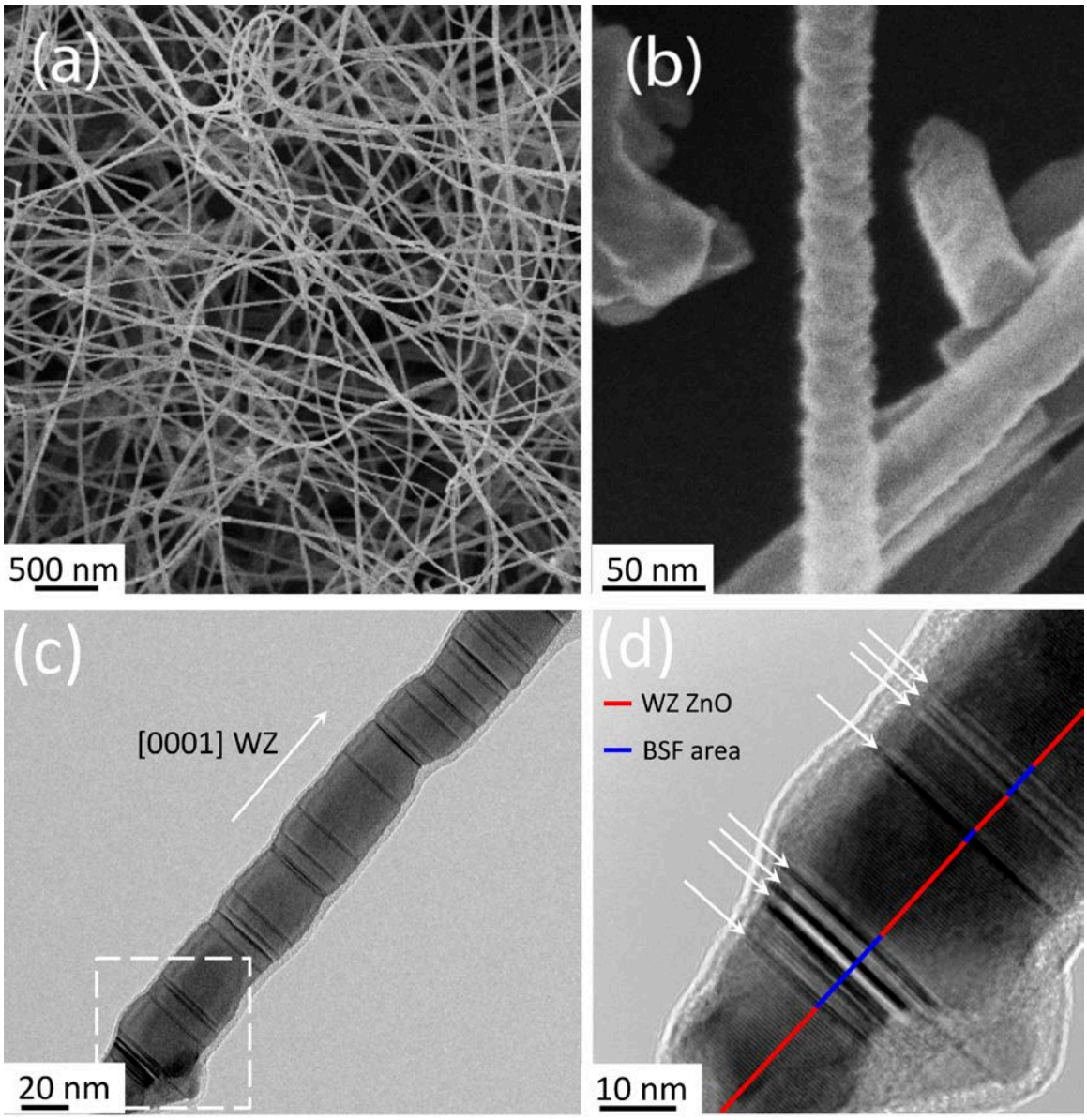

Fig. 2

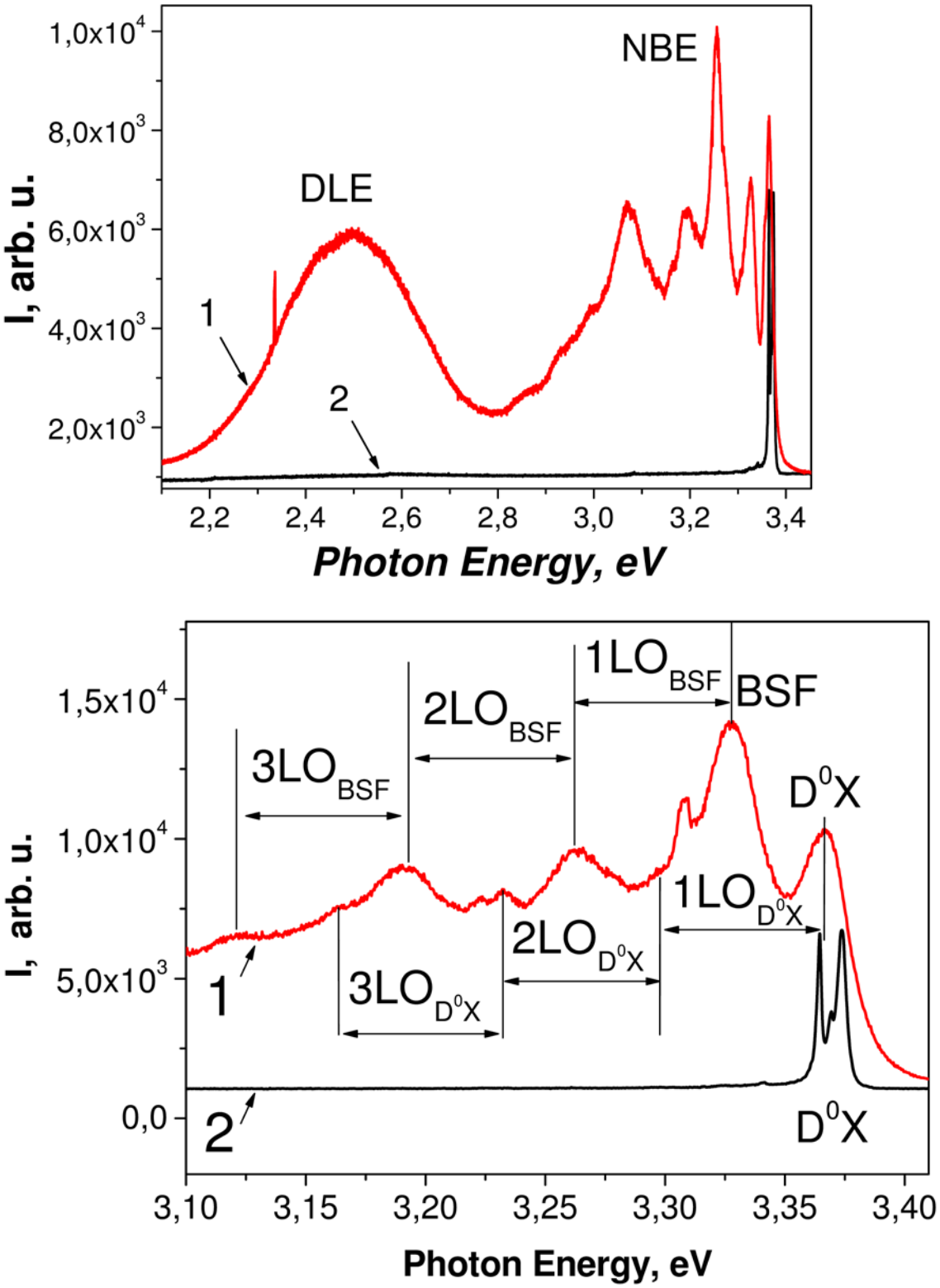
1,0x10^4
8,0x10^3
6,0x10^3
4,0x10^3
2,0x10^3
I, arb. u.
NBE
DLE
1
2
2,2
2,4
2,6
2,8
3,0
3,2
3,4
Photon Energy, eV
1,5x10^4
1,0x10^4
5,0x10^3
0,0
I, arb. u.
1LO BSF
BSF
2LO BSF
3LO BSF
D0X
1LO D0X
2LO D0X
3LO D0X
1
2
D0X
3,10
3,15
3,20
3,25
3,30
3,35
3,40
Photon Energy, eV

Fig. 3

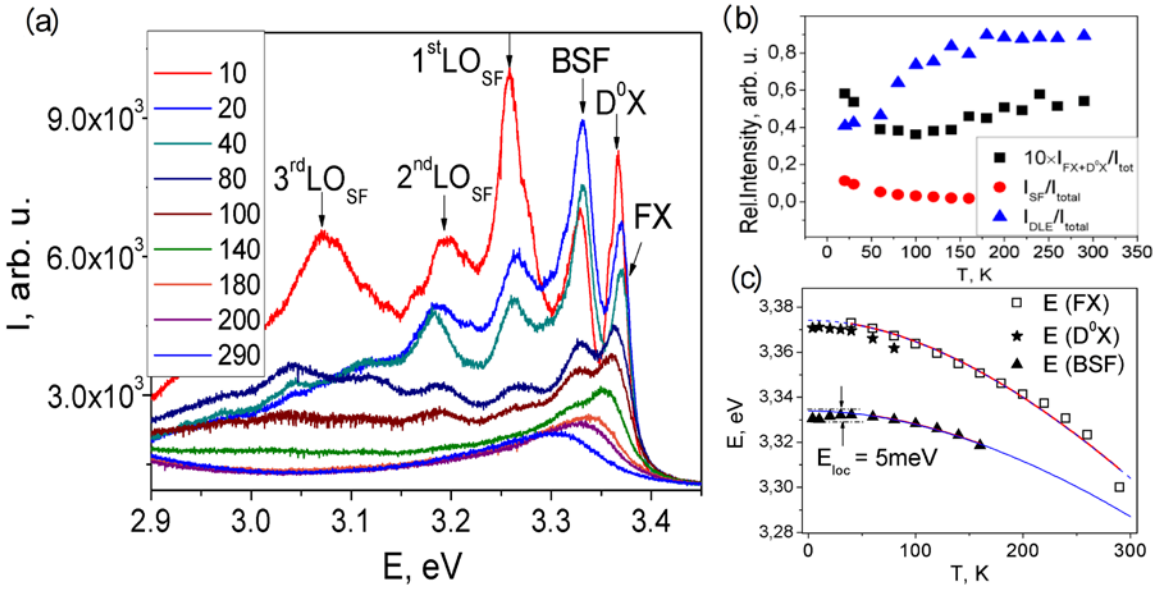
(a)
I, arb. u.
9.0x10^3
6.0x10^3
3.0x10^3
10
20
40
80
100
140
180
200
290
1st LO_SF
BSF
D^0X
3rd LO_SF
2nd LO_SF
FX
2.9
3.0
3.1
3.2
3.3
3.4
E, eV
(b)
Rel.Intensity, arb. u.
0,8
0,6
0,4
0,2
0,0
10×I_FX+D0X/I_tot
I_SF/I_total
I_DLE/I_total
0
50
100
150
200
250
300
350
T, K
(c)
E, eV
3,38
3,36
3,34
3,32
3,30
3,28
E (FX)
E (D^0X)
E (BSF)
E_loc = 5meV
0
100
200
300
T, K

Fig. 4

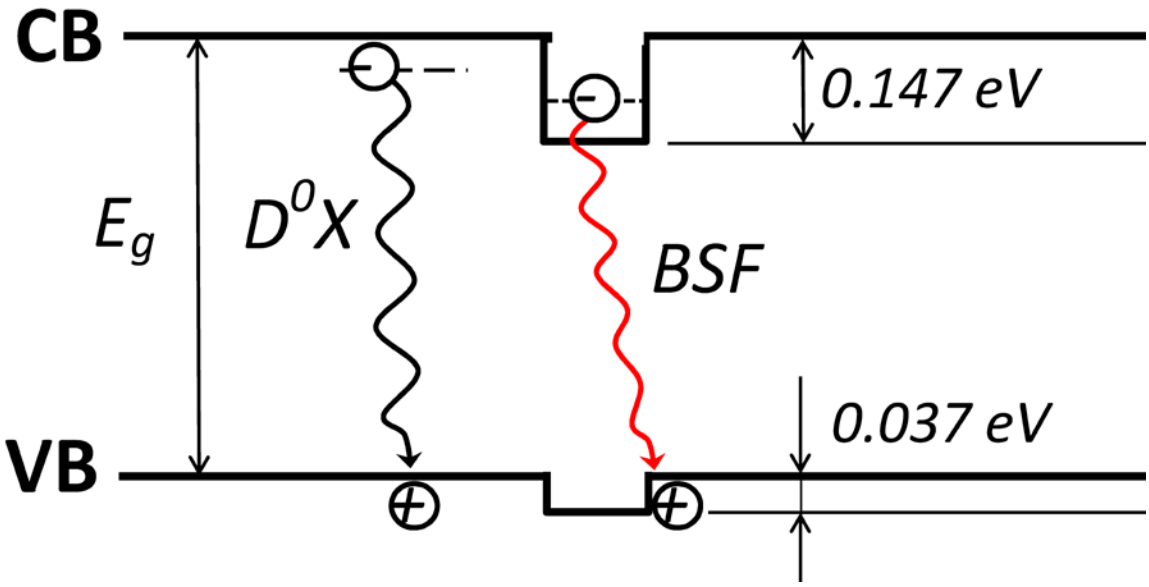
CB
VB
E_g
D^0X
BSF
0.147 eV
0.037 eV

Fig. 5